Supplementary information for :

High efficient large-scale preparation and electromagnetic property control of silica-NiFeP double shell composite hollow particles

Bin Liao,[a,b] Zhenguo An,[*,a] Jingjie Zhang[*,a]

[a]Technical Institute of Physics and Chemistry, Chinese Academy of Sciences, Beijing 100190 China.

[b]University of Chinese Academy of Sciences, Beijing 100049 , P. R. China.

Agents and factors (alkaline solution)	S1				S2				S3			
$NiSO_4 \cdot 6H_2O$	66.6				44.7				33.5			
$(NH_4)_2Fe(SO_4)_2 \cdot 6H_2O$	0				33.3				50			
$NaH_2PO_2 \cdot H_2O$	25				25				25			
$(NH_4)_2SO_4$	10				10				10			
$KNaC_4H_4O_6 \cdot 4H_2O$	75				75				75			
NH_2CH_2COOH	10				10				10			
PEG	10				10				10			
pH value	9				9				9			
temperature/℃	70				70				70			
Mole ratio(Fe^{2+}/(Fe^{2+}+Ni^{2+})	0				1:3				1:2			
Sample Names	**S11**	**S12**	**S13**	**S14**	**S21**	**S22**	**S23**	**S24**	**S31**	**S32**	**S33**	**S34**
Volume of solution(mL)	400	300	200	100	400	300	200	100	400	300	200	100
Mass of seeds(g)	4g	3/4**S11**	2/3**S12**	1/2**S13**	4g	3/4**S21**	2/3**S22**	1/2**S23**	4g	3/4**S31**	2/3**S32**	1/2**S33**

Table S1 Detailed chemical agent concentrations (g/L) and reaction conditions for different samples.

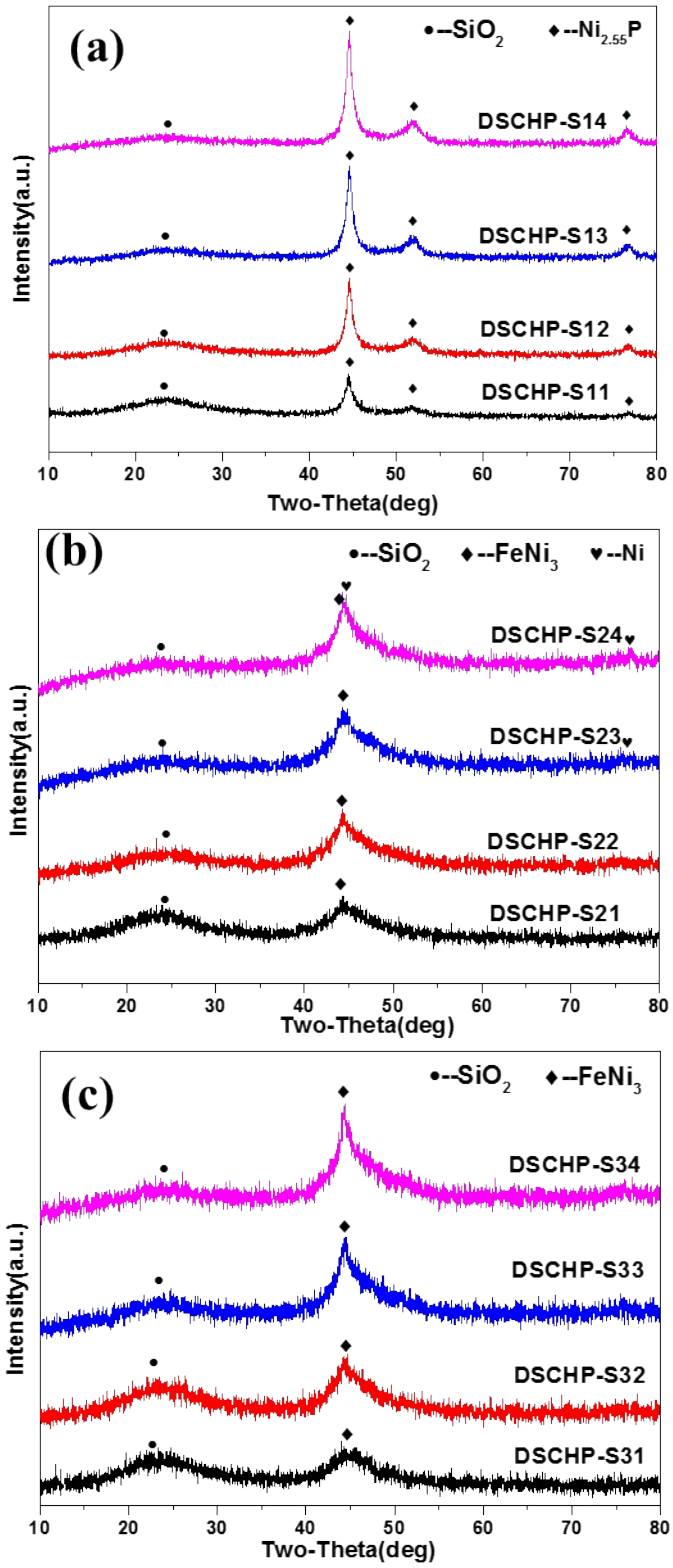

Fig. S1 XRD patterns of (a) DSCHP-S1, (b) DSCHP-S2 and (c) DSCHP-S3 with different plating times

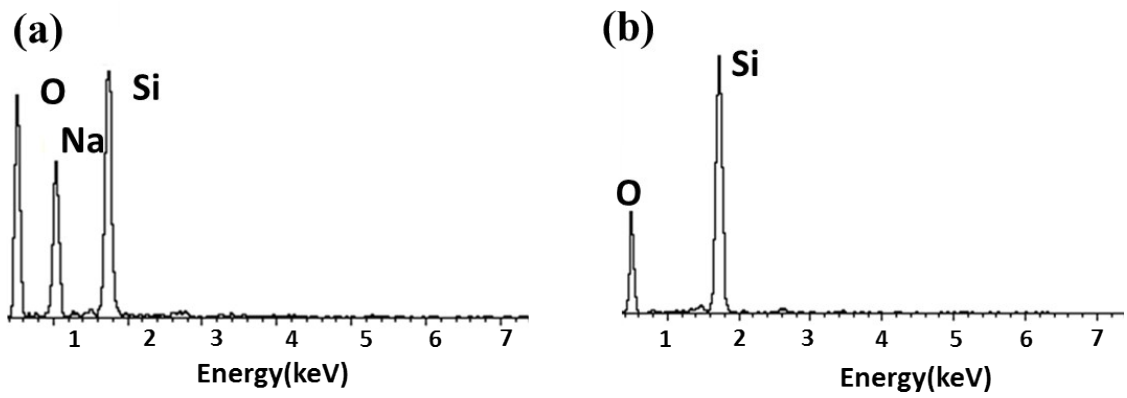

Fig. S2 EDX spectra of the obtained hollow particles with treatment (a) silane coupling and (b) sensitization

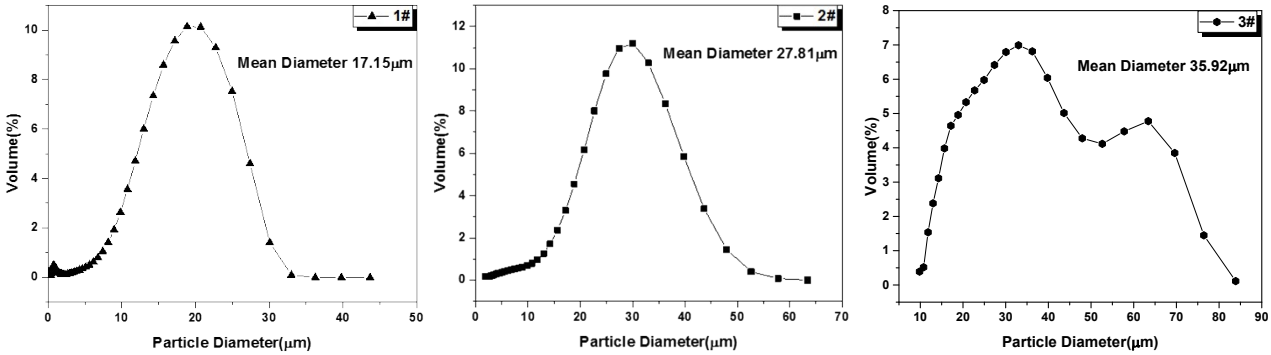

Fig. S3 Particle size distribution of obtained SSHPs with different parameter of spray drying.

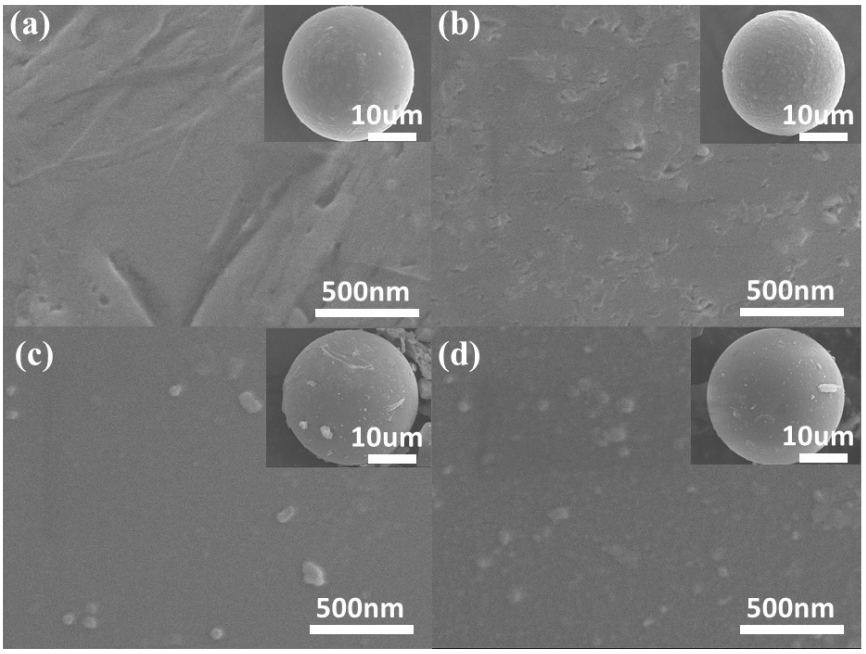

Fig. S4 SEM images of the hollow particles at different stage of pretreatments. (a) the pristine SSHPs, SSHPs obtained after silane coupling (b), sensitization (c) and activation (d).

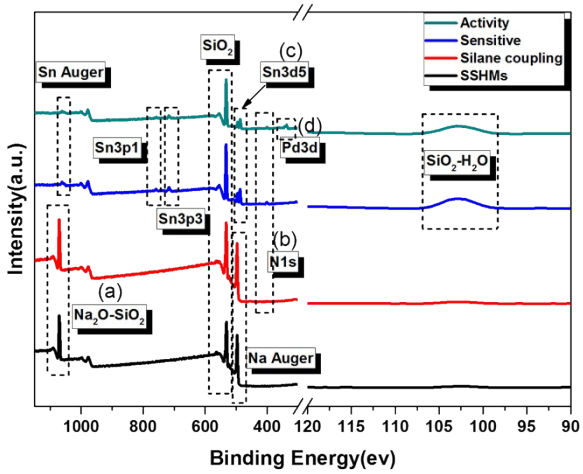

Fig. S5 XPS spectra of the SSHPs samples at different stage of pretreatment: (a) pristine SSHPs, (b) SSHPs after silane coupling, (c) SSHPs after activation.

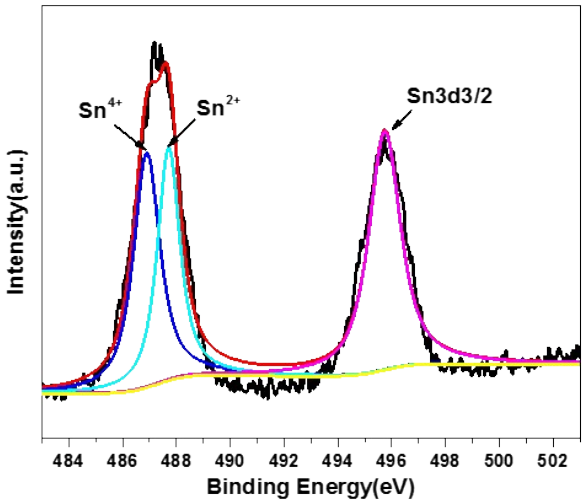

Fig. S6 XPS spectra of Sn3d for SSHPs after activation.

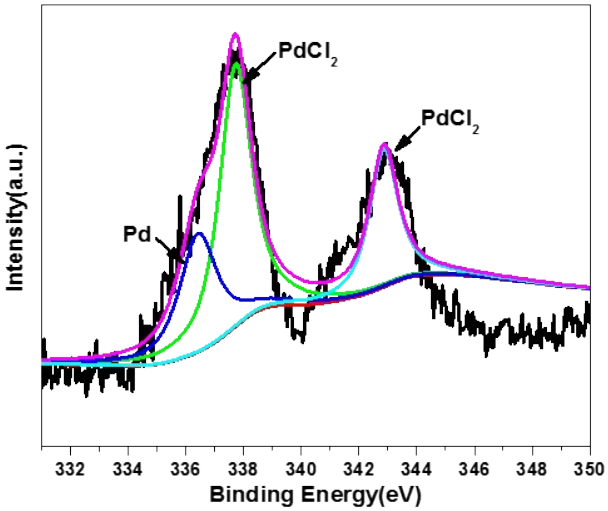

Fig. S7 XPS spectra of Pd3d for SSHPs after activation.

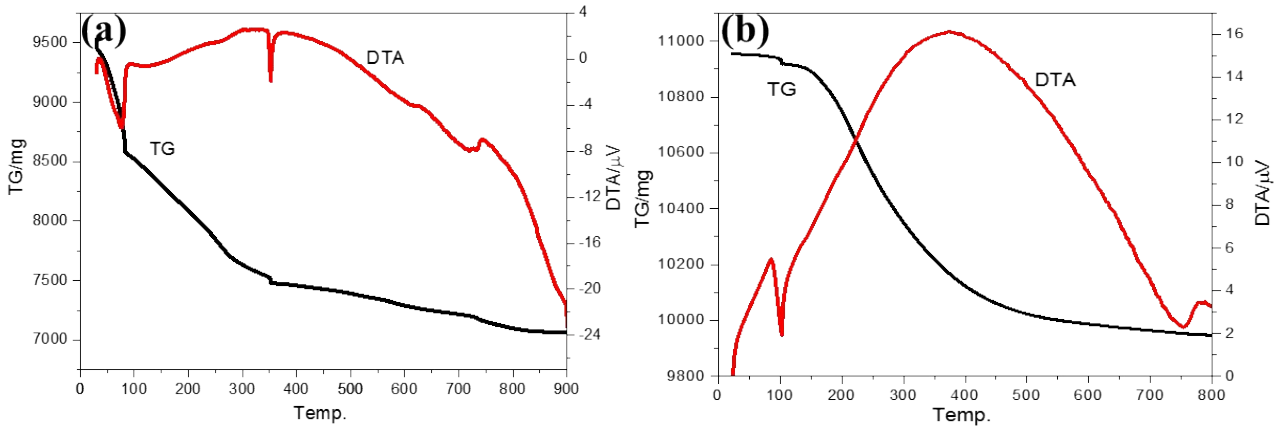

Fig. S8 TG-DTA curves of (a) SSHPs and (b) ASHPs.

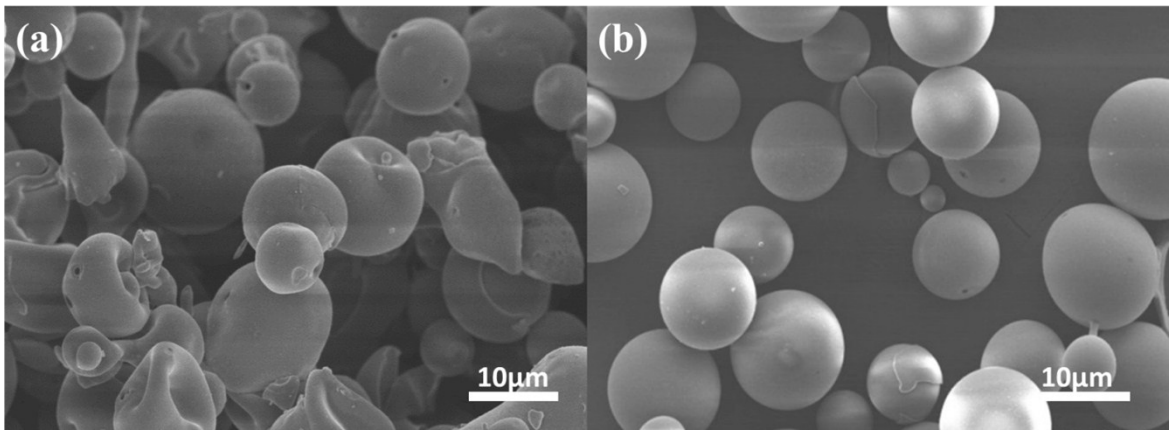

Fig. S9 SEM images of the pristine SSHPs calcinated at 400℃(a) and the ASHPs calcinated at 1300℃(b).

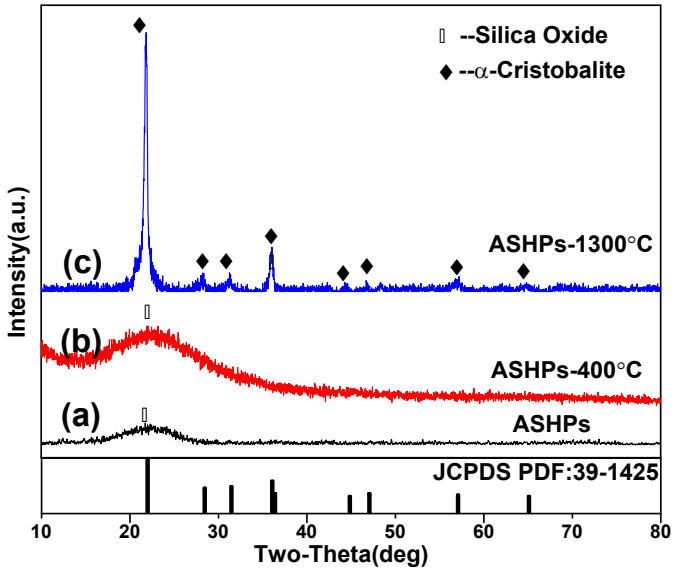

Fig. S10 XRD patterns of the ASHPs with heat treatment: (a)ASHPs, (b)400℃, and (c)1300℃

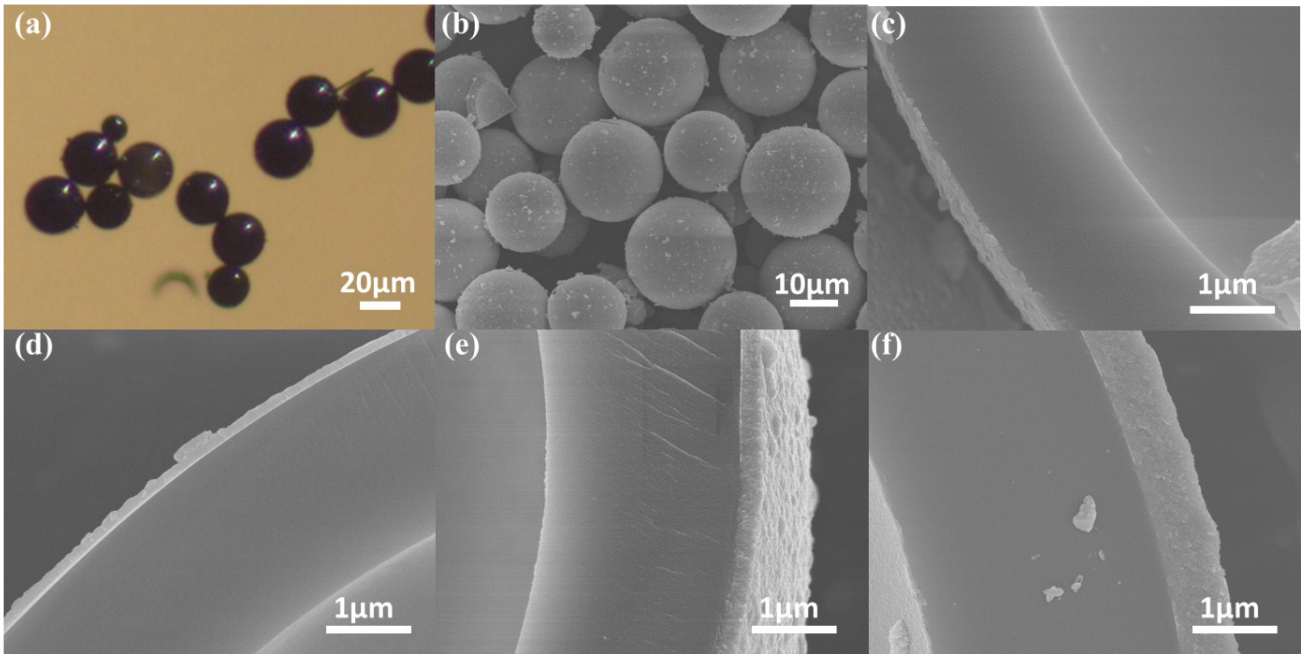

Fig. S11 (a) Optical microscopy image of DSCHP-S11 and SEM images of (b), (c) DSCHP-S11, (d) DSCHP-S12, (e)DSCHP-S13, (f)DSCHP-S14.

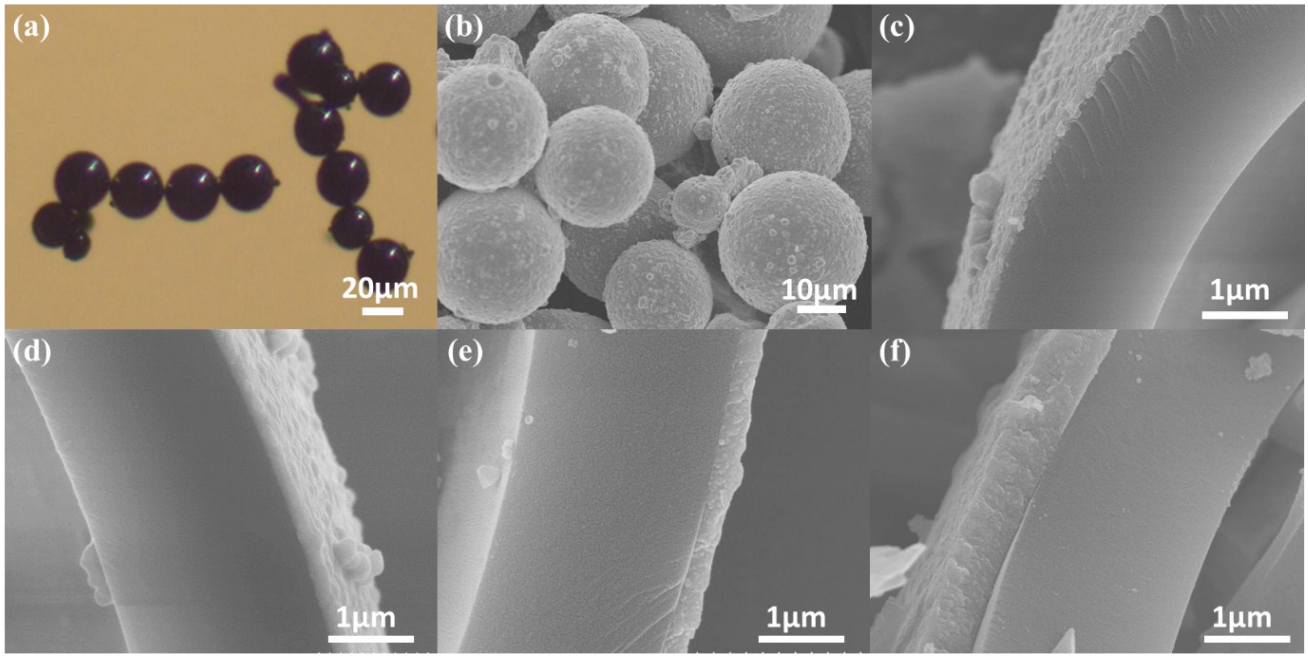

Fig. S12 (a) Optical microscopy image of DSCHP-S31 and SEM images of (b), (c) DSCHP-S31, (d) DSCHP-S32, (e)DSCHP-S33, (f)DSCHP-S34.

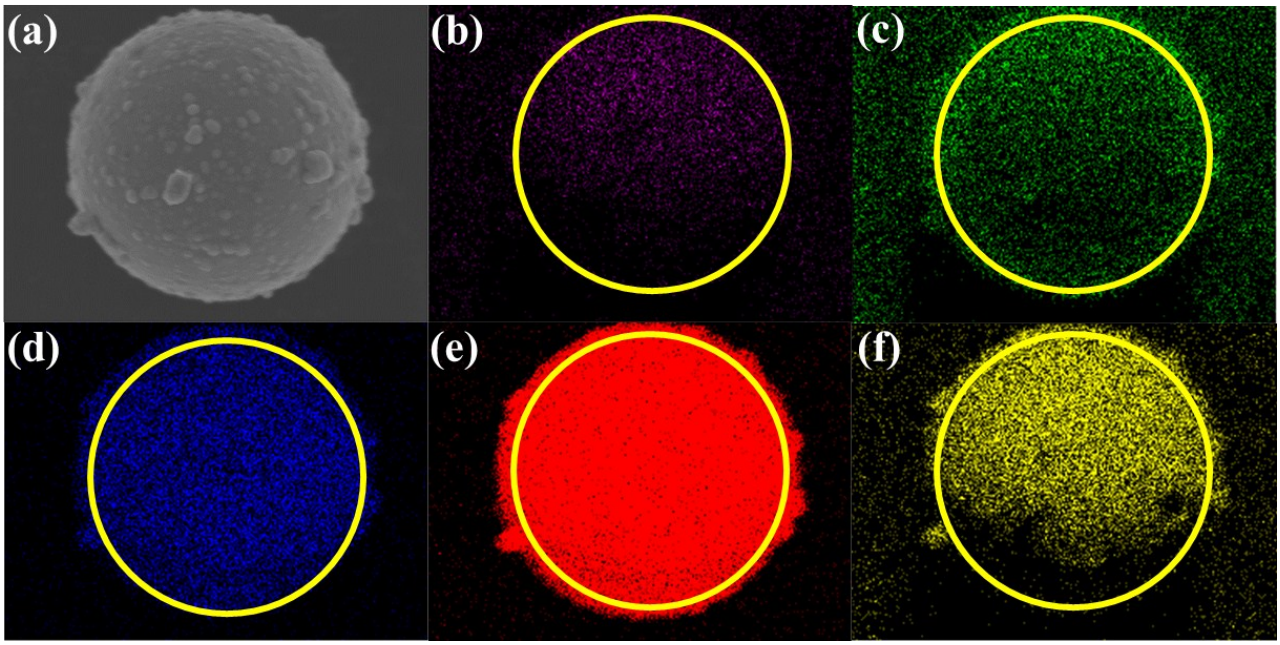

Fig. 13 SEM (a) image and the corresponding EDX element mapping of (b) Si, (c) O, (d) Fe and (e) Ni, and (f) P taken on a single particle of the as-obtained DSCHP-S23.

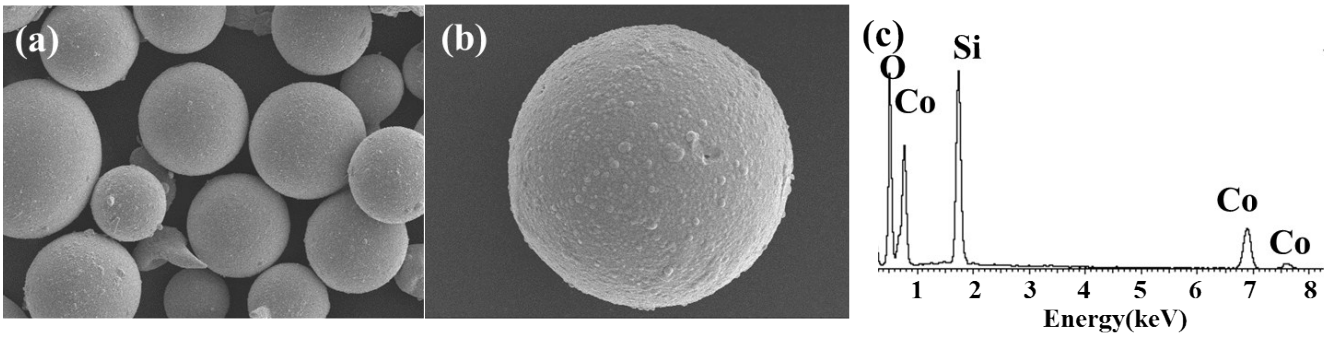

Fig. S14 (a), (b) SEM images and (c) EDX spectra of the as-obtained SiO_2-Co composite hollow particles.

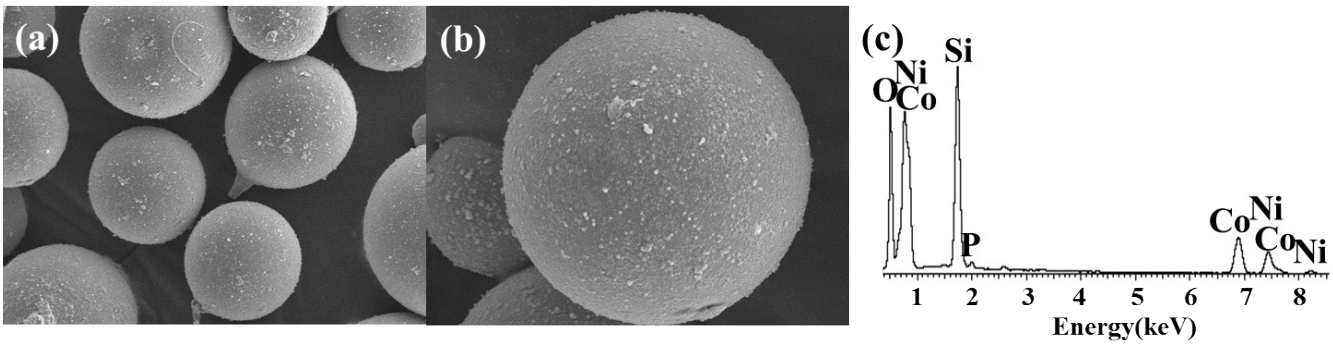

Fig. S15 (a), (b) SEM images and (c) EDX spectra of the as-obtained SiO_2- NiCoP composite hollow particles.

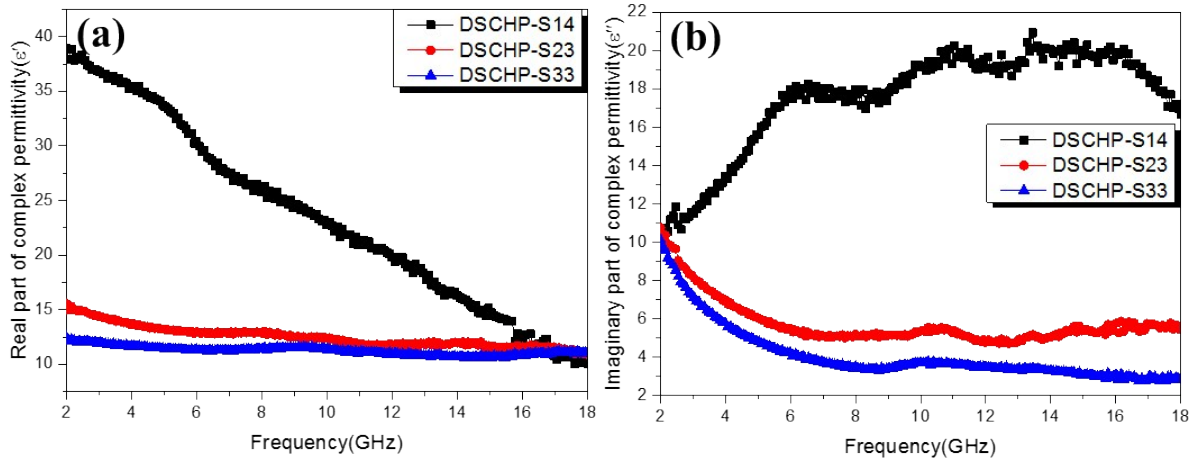

Fig. S16 The (a) real parts (ε`) and (b) imaginary parts (ε``) of DSCHP-S14 (black curve), DSCHP-S23 (red curve) and DSCHP-S33 (blue curve).

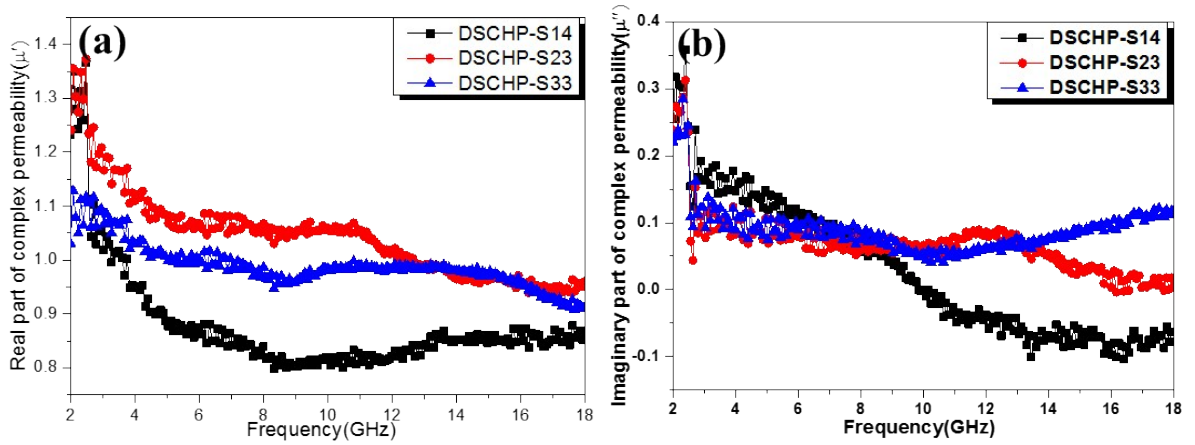

Fig. S17 The (a) real (μ`) and (b) imaginary (μ``) parts of the permeabilityof DSCHP-S14(black curve), DSCHP-S23(red curve) and DSCHP-S33(blue curve).

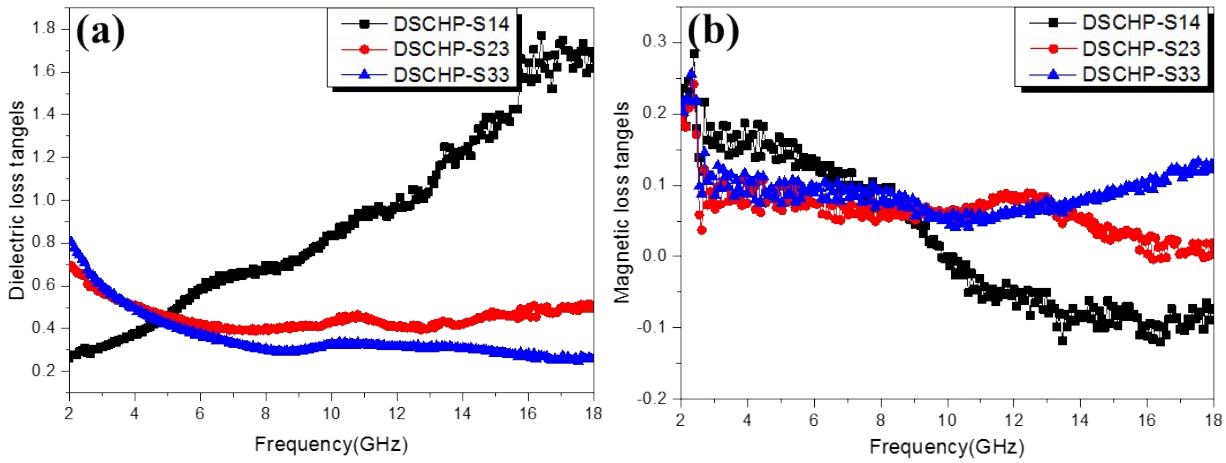

Fig. S18 Frequency dependences of the (a) dielectric loss tangent, (b) magnetic loss tangent

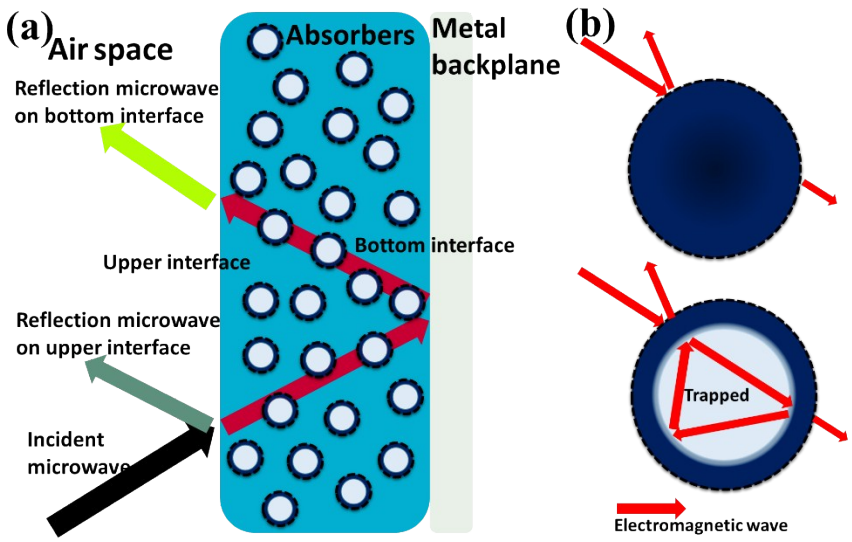

Fig. S19 The schematic diagram of electromagnetic microwave absorption mechanism for the DSCHPs. (a) electromagnetic wave incident to single-layer absorber baked by a metal backplane; (b) electromagnetic wave pathway illustration of solid structure and hollow structure.

Sample	Thickness (mm)	RL value (dB)	Bandwidth (RL<-10dB)(GHz)	Content (%)	Reference
Hollow ceramic-barium ferrites composite single shell microspheres	2.5	-10	<1	60	1
Hollow $CoFe_2O_4/Co_3Fe_7$ microspheres	2	-41.6	3	66.7	2
$CoFe_2O_4$ hollow sphere/graphene	2	-18.5	3.7	60	3
Co_3Fe_7/C nanoparticle	1.8	-26.8	2	50	4
FeCo/Graphene nanoparticle	2.5	-40.2	4	60	5
Hollow glass/nickel flowers microspheres	3.5	-15	0.8	30	6
NiCoP hollow spheres	2.5	-41.7	2	40	7
Silica@Iron microcubes	4.5	-54	1.5	55	8
Ni-15%Fe coated microspheres	5	-25	<1	50	9
Co–Co_3O_4 hybrid hollow sphere	5	-18.5	<1	30	10
C@Ni-NiO solid sphere	5	-10	<1	30	11
Hollow glass/Ni thin film	3	-35	1	37.5	12
DSCHPs-S23	1.75	-16.46	3.2	30	This work
DSCHPs-S33	1.5	-45.9	4	30	This work

Table S2. The electromagnetic absorption properties of similar samples

Reference

1 X. Cai, J. Wang, R. Yang, C. Xiong, H. Lou, *Int. J. Appl. Ceram. Technol.,* 2015, ***12***, 8.
2 W. Li, L. Wang, G. Li, Y. Xu, *J. Magn. Magn. Mater*., 2015, ***377***, 259.
3 M. Fu, Q. Jiao, Y. Zhao, H. Li, *J. Mater. Chem. A*, 2014, ***2***, 735.
4 X. D. Guo, X. J. Qiao, Q. G. Ren, X. Wan, W. C. Li, Z. G. Sun, *Appl. Phys. A*, 2015, ***120***, 43.
5 X. Li, J. Feng, Y. Du, J. Bai, H. Fan, H. Zhang, Y. Peng, F. Li, *J. Mater. Chem. A*, 2015, ***3***, 5535.
6 Z. An, S. Pan, J. Zhang, *J. Phys. Chem. C*, 2009, ***113***, 2715.
7 Z. Li, Y. Deng, B. Shen, L. Liu, W. Hu, *J. Alloy. Compd.*, 2010, ***491***, 406.
8 Z. Yang, Z. Li, L. Yu, Y. Yang, Z. Xu, *J. Mater. Chem. C*, 2014, ***2***, 7583.
9 S. T. Kim, S. S.Kim, *J. Appl. Phys.*, 2014, ***115***, 17A528.
10 H. Wu, Q. Wu, L. Wang, *Mater. Charact.*, 2015, ***103***, 1.
11 H. Wu, G. Wu, Q. Wu, L. *Mater. Charact.*, Wang, 2014, ***97***, 18.
12 Z. W. Liu, L. X. Phua, Y. Liu, C. K. Ong, *J. Appl. Phys.*, 2006, ***100***, 093902.

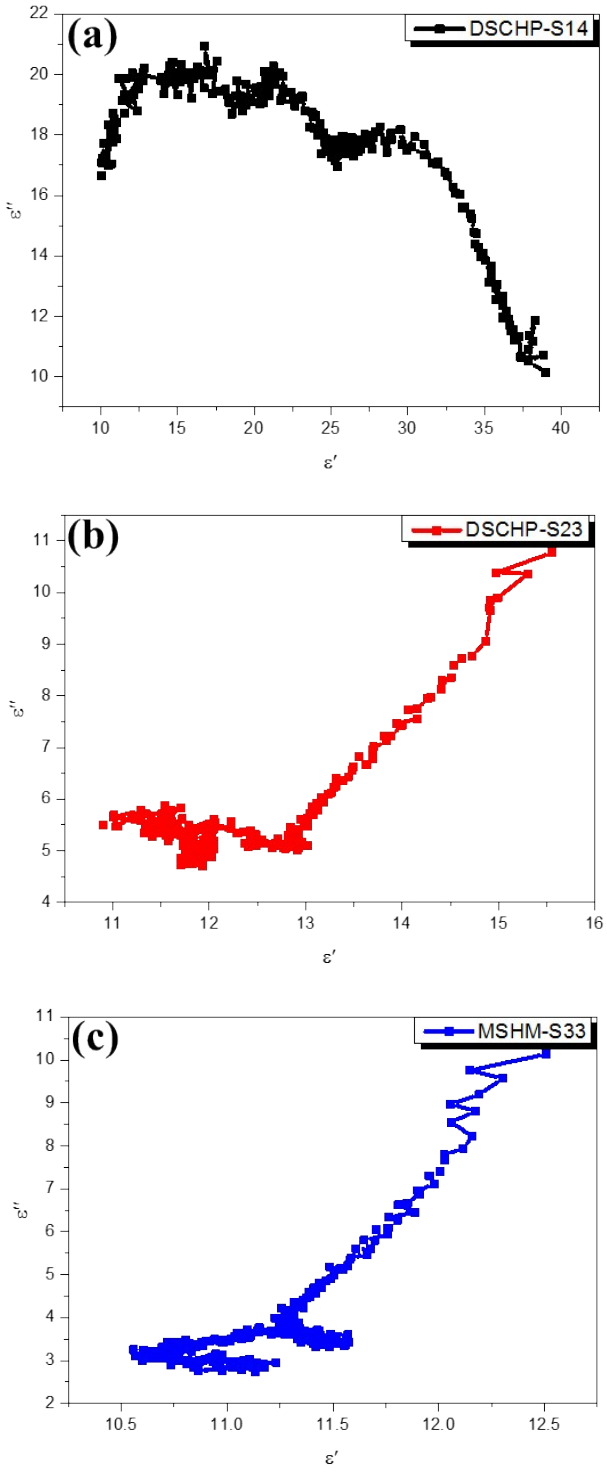

Fig. S20 Typical Cole-Cole semicircles for (a) DSCHP-S14, (b) DSCHP-S23 and (c) DSCHP-S33.